Numerical Simulations on Geometrical Properties of Wall-attaching Transonic Jet

Hu Dapeng, Chen Zuzhi, Dai Yuqiang, Chen Shengtao
(Gas Wave Refrigeration Research and Popularization Center of Dalian University of Technology, Dalian 116012, China)

Abstract: Effects of operating conditions and device's geometrical sizes on geometrical properties of wall-attaching transonic jet between two parallel plat plates are numerically simulated. Conclusions are as follows: 1) Upriver part of the wall-attaching jet's center streamline is in good accordance with parabola; 2) When both gas inlet pressure and outlet pressure as well as their ratio are not too high (the outlet pressure is less than 10 MPa and the pressure ratio is less than 3), the center streamlines of the wall-attaching jet with the same pressure ratio coincide with each other very well, and the deflection degree of the center streamline decreases with rise of the pressure ratio; 3) The deflection degree of the jet's center streamline decreases with either broadening of nozzle's throat or rise of wall offset; 4) With rise of the pressure ratio, attachment distance of the jet increases, but the increase rate descends; 5) The attachment distance ascends with rise of either the nozzle's throat or the wall offset.

Key words: wall-attaching transonic jet; parallel plat plates; geometrical properties; attachment distance

1 Introduction

As shown in Fig. 1 (a), when jet flows between two parallel plat plates, it will deflect and attach to one wall firmly. This phenomenon of jet was firstly discovered by Coanda, a French engineer, and called Coanda effect[1]. Wall-attaching jet has some special properties, such as high heat transfer rate and high

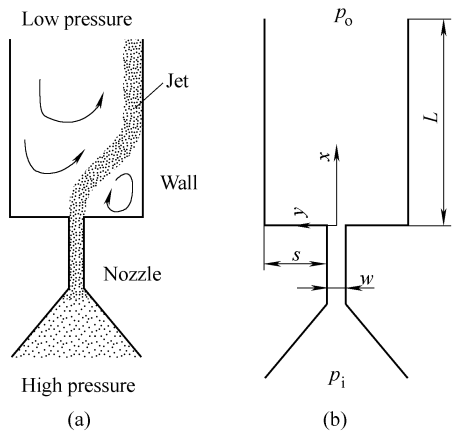

Fig. 1 Schematic diagram of wall-attaching jet

turbulence intensity, which have been utilized in practice. Based on wall-attaching jet, static gas wave refrigerator (SGWR)[2], a new type refrigerator of compressed gas, was developed, in which oscillation of the jet was result of the wall-attaching jet's periodic switch from one wall to the other caused by pressure or momentum signal imported through hole in the wall. During engineering design, the wall-attaching jet's geometrical properties including deflection degree, attachment distance and shape of the jet's center streamline, are usually needed to be calculated, which are affected by operating pressure (p_i and p_o), width of nozzle (w), wall offset (s) and wall length (L) displayed in Fig. 1(b).

The wall-attaching jet has been studied mainly by experiments aimed at subsonic gas[3-5]. There are several configuration analysis models based on a number of hypotheses[6]. Flow field of transonic wall-attaching jet is more complicated than that of the subsonic jet and it is hard to test its flow parameters. In this paper, flux vector splitting algorithm on the basis of van Leer's scheme[7] is introduced to compute flow field of the wall-attaching jet between two parallel plat plates. Effects of the operating pressure and device's geometrical sizes on geometrical properties are studied. Air serves as working medium.

2 Mathematical Model and Numerical Methods

2.1 Mathematical Model

Ratio of flow channel's depth to width is great and effects of turbulence and viscosity can't be neglec-

Received 14 *December* 2006

ted. Therefore, two-dimensional Navier-Stokes equations (farve averaged)[8] are adopted to model flow in this paper. The equations are expressed in integral notation as follows:

$$\frac{\mathrm{d}}{\mathrm{d}t}\int \boldsymbol{W}\mathrm{d}A_{\mathrm{f}} + \int (\nabla\cdot \boldsymbol{F}_{\mathrm{C}})\,\mathrm{d}A_{\mathrm{f}} = \int (\nabla\cdot \boldsymbol{F}_{\mathrm{D}})\,\mathrm{d}A_{\mathrm{f}} \quad (1)$$

Where $\boldsymbol{W}$ represents variable vector, and $\boldsymbol{F}_{\mathrm{C}}$ and $\boldsymbol{F}_{\mathrm{D}}$ represent convection flux and diffusion flux respectively.

$$\boldsymbol{W} = \begin{bmatrix} \rho \\ \rho u \\ \rho v \\ E \end{bmatrix}, \boldsymbol{F}_{\mathrm{C},(x)} = \begin{bmatrix} \rho u \\ \rho uu + p \\ \rho uv \\ (E+p)u \end{bmatrix},$$

$$\boldsymbol{F}_{\mathrm{D},(x)} = \begin{bmatrix} 0 \\ \tau_{xx} - \frac{2}{3}\rho k \\ \tau_{xy} \\ u\tau_{xx} + v\tau_{xy} + (\lambda + \lambda_t)\frac{\partial T}{\partial x} \end{bmatrix} \quad (2)$$

$F_{C(y)}$ and $F_{D(y)}$ can be written in similar fashion.

In above expressions

$$E = \rho\left[e + \frac{1}{2}(u^2 + v^2)\right] \quad (3)$$

$$\tau_{xx} = -\frac{2}{3}(\mu + \mu_t)(\nabla\cdot \boldsymbol{V}) + 2(\mu + \mu_t)\frac{\partial u}{\partial x} \quad (4)$$

$$\tau_{xy} = \tau_{yx} = (\mu + \mu_t)\left(\frac{\partial u}{\partial y} + \frac{\partial v}{\partial x}\right) \quad (5)$$

$$\tau_{yy} = -\frac{2}{3}(\mu + \mu_t)(\nabla\cdot \boldsymbol{V}) + 2(\mu + \mu_t)\frac{\partial v}{\partial y} \quad (6)$$

The $k-\varepsilon$ model is chosen to simulate turbulence. Following formulas are used to calculate the turbulent viscosity and the turbulent thermal conductivity:

$$\mu_t = \frac{C_\mu k^2 \rho}{\varepsilon}, \lambda_t = \frac{\mu_t c_{\mathrm{p}}}{Pr_t}, Pr_t = 0.9 \quad (7)$$

The $k-\varepsilon$ equations are as follows:

$$\frac{\partial(\rho k)}{\partial t} + \frac{\partial}{\partial x_j}(\rho u_j k) = P - \rho\varepsilon + \frac{\partial}{\partial x_j}\left[\left(\mu + \frac{\mu_t}{\sigma_k}\right)\frac{\partial k}{\partial x_j}\right] \quad (8)$$

$$\frac{\partial(\rho\varepsilon)}{\partial t} + \frac{\partial}{\partial x_j}(\rho u_j \varepsilon) = C_{\varepsilon_1}\frac{P\varepsilon}{k} - C_{\varepsilon_2}\frac{\rho\varepsilon^2}{k} + \frac{\partial}{\partial x_j}\left[\left(\mu + \frac{\mu_t}{\sigma_\varepsilon}\right)\frac{\partial \varepsilon}{\partial x_j}\right] \quad (9)$$

where:

$$P = \mu_t\left(\frac{\partial u_i}{\partial x_j} + \frac{\partial u_j}{\partial x_i} + \frac{2}{3}\nabla\cdot \boldsymbol{V}\delta_{ij}\right)\frac{\partial u_i}{\partial x_j} - \frac{2}{3}\nabla\cdot \boldsymbol{V} \quad (10)$$

C_μ, σ_k, σ_ε, $C_{\varepsilon 1}$, $C_{\varepsilon 2}$ are all experiential constants, whose valves are listed in Table 1.

Table 1 Experiential constants

C_μ	σ_k	σ_ε	$C_{\varepsilon 1}$	$C_{\varepsilon 2}$
0.09	1	1.3	1.44	1.92

In the near-wall region, wall-functions as follows are used to compute k and ε

$$k = \frac{\mu_\tau^2}{\sqrt{C_\mu}}, \varepsilon = \frac{C_\mu^{\frac{3}{4}} k^{\frac{3}{2}}}{\kappa y} \quad (11)$$

There are three types of boundaries: high pressure gas inlet port, jet outlet port and static wall. All walls are supposed to be adiabatic

2.2 Numerical Methods

Composite structured grid is adopted to discretize computational space. Finite volume method[9] is introduced to discretize control equations. After discretized, equation (1) is transformed into equation (12):

$$\frac{\Delta W}{\Delta t}\Delta A_{\mathrm{f}} + \sum_{n=1}^{N_{\mathrm{face}}}\left[(\boldsymbol{F}_{\mathrm{C}} - \boldsymbol{F}_{\mathrm{D}})\Big|_{\mathrm{f}}^{\mathrm{n}}\right]\cdot \hat{n}_f^{n+1}\cdot \Delta h = -\sum_{n=1}^{N_{\mathrm{face}}}\left[\left(\frac{\partial \boldsymbol{F}_{\mathrm{C}}}{\partial W} - \frac{\partial \boldsymbol{F}_{\mathrm{D}}}{\partial W}\right)\Big|_{\mathrm{f}}^{n}\Delta W\cdot \hat{n}_f^{n+1}\cdot \Delta h\right] \quad (12)$$

$\frac{\partial \boldsymbol{F}_{\mathrm{C}}}{\partial W}$ and $\frac{\partial \boldsymbol{F}_{\mathrm{D}}}{\partial W}$, respectively, represent convection flux Jacobian and diffusion flux Jacobian. van Leer's scheme[9] is used to discretize convection flux. Central differencing scheme is used to discretize diffusion flux.

On the gas inlet port boundary (+), the total pressure and temperature are held constant:

$$p^+\left(1 + \frac{k-1}{2}M^{+2}\right)^{\frac{k}{k-1}} = p_0\left(1 + \frac{k-1}{2}M_0^2\right)^{\frac{k}{k-1}}$$
$$T^+\left(1 + \frac{k-1}{2}M^{+2}\right) = T_0\left(1 + \frac{k-1}{2}M_0^2\right) \quad (13)$$

and the remaining flow parameters are calculated based on the interior conditions and isoentropy conditions. On the jet outlet port, the inflow-outflow condition is used[10]. All the walls are supposed to be adiabatic and the boundary conditions are:

$$u^+ = 0, v^+ = 0, T^+ = T_0, p^+ = p_0 \quad (14)$$

3 Results and Discussion

In actual physical process, the jet's attachment is caused mainly by asymmetry of the device. The symmetrical devices are adopted in the current numerical simulation and it is the asymmetry of the computing process which induces the jet's deflection and attaching to wall.

Simulated flow field is shown in Fig. 2, from which entrainment phenomena of the jet can be seen

clearly. An eddy zone with low pressure is produced between the jet and the attached wall, and is isolated to the low pressure gas outlet port by the jet. The other side of the jet is opened to the gas outlet port, and there exists small pressure difference between them. The jet is forced to attach to the wall firmly as a result of pressure difference between two sides of the jet.

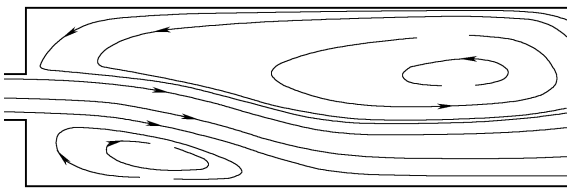

Fig. 2 Streamlines between two plat plates (p_i = 0.2 MPa, p_o = 0.1 MPa, w = 2 mm, s = 3 mm, L = 25 mm)

Fig. 3 shows computed geometrical configuration of the wall-attaching jet, from which it can be seen that after ejected from the nozzle, the jet gradually deflects and steadily attaches to one wall at last. Center streamline is the streamline which originates from center of the nozzle. A denotes attachment distance. Parabola is introduced to fit simulated upriver part of the center streamline, and the result is illustrated in Fig. 4 from which we can see that the corresponding part of the jet accords with parabola very well.

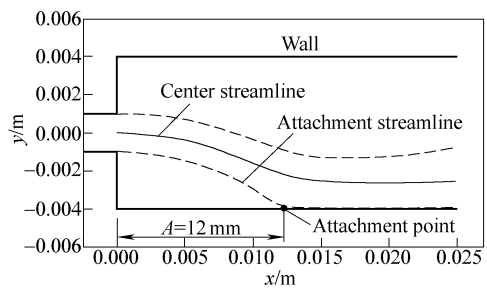

Fig. 3 Geometrical configuration of wall-attaching jet(p_i = 0.2 MPa, p_o = 0.1 MPa, w = 2 mm, s = 3 mm, L = 25 mm)

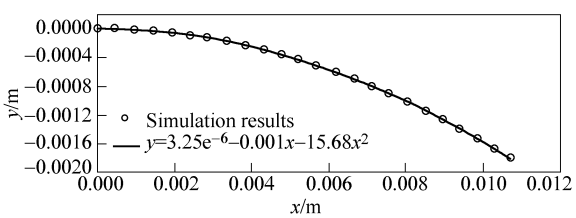

Fig. 4 Center streamline of the wall-attaching jet

1) Center streamlines of wall-attaching jet with different operating pressure and geometrical sizes

Fig. 5 exhibits streamlines with different operating pressure. The figure reveals that the streamlines nearly overlap with each other with the same ratio of the inlet pressure to the outlet pressure ($\omega = p_i/p_o$), and that deflection degree of the jet decreases with rise of ω. The deflection degree of the wall-attaching jet is determined by both the pressure difference between two sides of the jet and the jet's momentum flux. It increases with rise of the pressure difference but decreases with that of momentum flux. When the gas outlet pressure is fixed, both the pressure

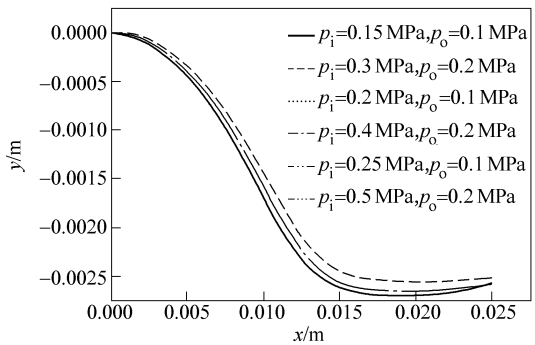

Fig. 5 Center streamline of the wall-attaching jet with different operating pressure (w = 2 mm, s = 3 mm, L = 25 mm)

difference and the momentum of the jet increase with rise of the ratio. Under that condition, the deflection degree of the jet is mainly influenced by the jet's momentum flux and ascends with rise of it. If either the pressure ratio or the operating pressure value is too high (the ratio exceeds 3, the outlet pressure exceeds 10 MPa), the results shown in Fig. 5 can't be obtained.

Fig. 6 displays center streamlines with different width of the nozzle's throat, from which it can found out that the jet's deflection degree descends with rise of the width. With constant inlet pressure and outlet pressure, the jet's momentum flux is in direct proportion to the width of nozzle's throat, but the pressure difference between two sides of the wall-attaching jet ascends only a little with rise of the width. Hence, the deflection degree decreases.

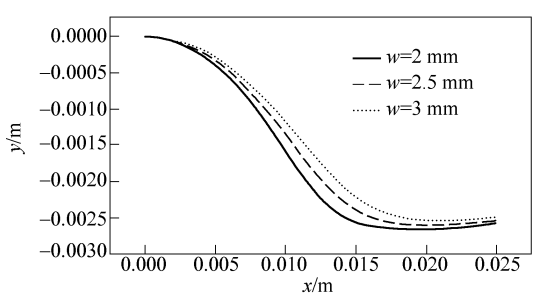

Fig. 6 Center streamlines of the wall-attaching jet with different width of nozzle's throat (ω = 2, s = 3 mm, L = 25 mm)

As Fig. 7 illustrates, the jet's deflection degree ascends appreciably with decrease of the wall offset, which is due to decrease of the pressure difference between two sides of the jet.

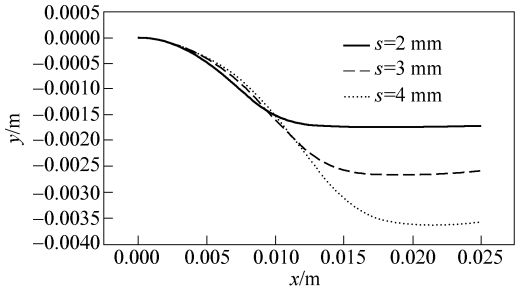

Fig. 7 Center streamline of the wall-attaching jet with different wall-offset
($\omega = 2$, $w = 2$ mm, $L = 25$ mm)

Fig. 8 shows center streamlines of wall-attaching jet with different wall length. It can be found out that the wall length has little effect on the jet's deflection degree. When both gas inlet pressure and outlet pressure are fixed, the pressures on both sides of the wall-attaching jet decrease with rise of the wall length, but their difference hardly varies. Under the condition of constant operating pressure, the jet's momentum flux doesn't change. Therefore, the deflection degree of jet doesn't change too.

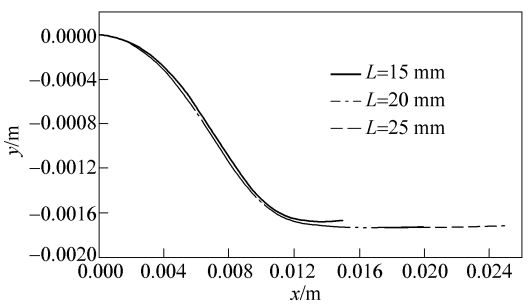

Fig. 8 Center streamline of the wall-attaching jet with different length of the walls
($\omega = 2$, $w = 2$ mm, $s = 3$ mm)

2) Attachment distance with different operating pressures and geometrical sizes

Along with the jet flowing downstream, the gas expands and the jet's width increases. When the wall offset is great, effect of the jet's width increase on the attachment distance can be neglected. However, with small wall offset, effect of the wall offset can't be neglected and the attachment distance of the wall-attaching jet is determined by both the jet's deflection degree and width increase of the jet.

Fig. 9 exhibits simulated attachment distance with different operating pressure, from which we can find out that although center streamlines accord with each other with the same ω, the attachment distances (A) are not equal to each other. The reason is that attachment distance is affected not only by the jet's deflection degree but also by the jet's width whose variation with the jet developing downstream is influenced by either the pressure ratio or the pressure value. In Fig. 9, when the ratio is equal to 2, the attachment distances approach to each other. Fig. 10 displays how the pressure ratio influences the attachment distance, from witch we can see that when the ratio is less than 2, the attachment distance increases notably with ω since it is determined mainly by the jet's deflection degree. However with rise of the pressure ratio, the increase rate of the attachment distance descends. The attachment distance with the ratio equal to 2.2 is very close to that with the ratio equaling to 2.5. Under this condition the attachment distance is determined mainly by the jet's expansion. From Fig. 9, it can be seen that with different pressure ratio, the trends of the attachment distance's variations with the gas outlet pressure are different. The reason is that with different pressure ratio the trends of the attachment streamlines' variation are different.

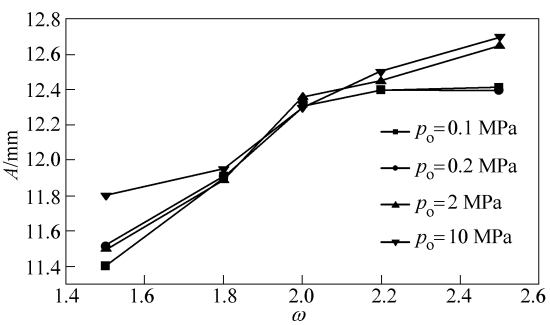

Fig. 9 Attachment distance with different operating pressure($w = 2$ mm, $s = 3$ mm, $L = 25$ mm)

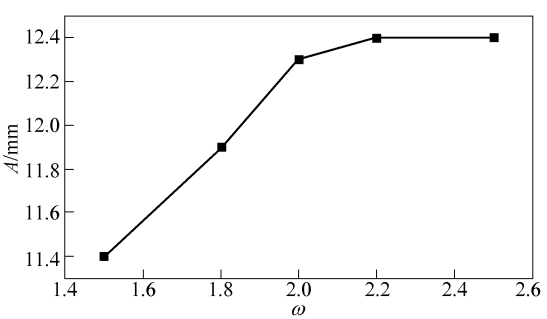

Fig. 10 Effect of the ratio of gas inlet pressure to outlet pressure on attachment distance
($p_o = 0.1$ MPa, $w = 2$ mm, $s = 3$ mm, $L = 25$ mm)

Fig. 11 and 12 respectively show impacts of the

width of the nozzle's throat and the wall offset, from which it can be seen that the attachment distance increases with rise of either the nozzle throat's width or the wall offset. The reason is similar to that why the deflection degree ascends with rise of them.

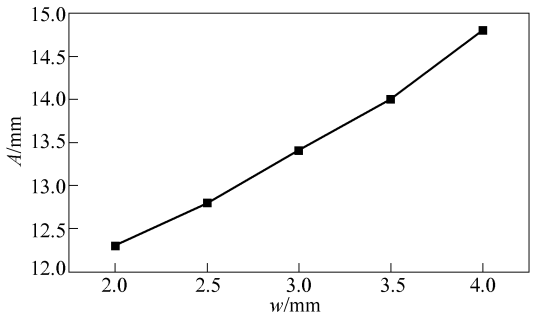

Fig. 11 Effect of width of nozzle's throat on attachment distance (p_i = 0.2 MPa, p_o = 0.1 MPa, s = 3 mm, L = 25 mm)

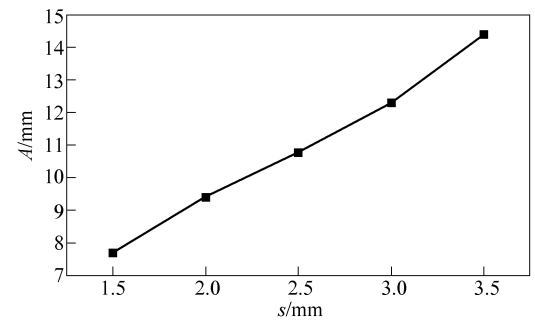

Fig. 12 Effect of the wall offset on attachment distance (p_i = 0.2 MPa, p_o = 0.1 MPa, w = 2 mm, L = 25 mm)

4 Conclusions

The wall-attaching jet between two plat plates is numerically investigated in the current paper. Emphasis is placed on discussing effects of the operating conditions and the device's geometrical sizes on the jet's geometrical properties. Conclusions are drawn as follows: 1) The upriver part of the center streamline of the wall-attaching jet is in good accordance with parabola; 2) When both the gas inlet pressure and the outlet pressure as well as their ratio are not too high (the outlet pressure is less than 10 MPa and the pressure ratio is less than 3), the center streamlines of the jet with the same pressure ratio coincide with each other very well, and the deflection degree of the center streamline decreases with rise of the pressure ratio; 3) The deflection degree of the jet's center streamline decreases with either broadening of the nozzle's throat or rise of the wall offset; 4) The attachment distance of the wall-attaching jet increases with rise of the pressure ratio but the rate of the increase descends; 5) The attachment distance ascends with rise of either the nozzle's throat or the wall offset.

References

[1] Coanda H. Device for deflecting a stream of elastic fluid projected into an elastic fluid [P]: US: 2052869. 1936

[2] Hu Dapeng. Research on Static Thermal Separator [D]. Dalian: Dalian University of Technology. 1989. (in Chinese)

[3] Bourque C, Newmann G. Reattachment of a two-dimensional incompressible jet to an adjacent flat plate [J]. Aeron Quarterly, 1960, 11: 201 - 232

[4] Lai J C S, Lu D. Effect of wall inclination on the mean flow and turbulence characteristics in a two-dimensional wall jet [J]. International Journal of Heat and Fluid Flow, 1996, 17(4): 377 - 385

[5] Song H B, Yoon S H, Lee D H. Flow and heat transfer characteristics of a two-dimensional oblique wall attaching offset jet [J]. Heat and Mass Transfer, 2000, 43:2395 - 2404

[6] Lu Runlin, Guo Bingrong (translating). Jet Engineering [M]. Beijing: Science Press, 1977. (in Chinese)

[7] van Leer B. Flux - vector splitting for the Euler equations [R]. Lecture Notes in Phys, 1982

[8] Zhang Zhaoshun, Cui Guixiang, Xu Chunxiao. Theory and Modeling of Turbulence [M]. Beijing: Tsinghua University Press, 2005 (in Chinese)

[9] Tao Wenquan. Numerical Heat Transfer [M]. Xi'an: Xi'an Jiaotong University Press, 2001. (in Chinese)

[10] Wu Ziniu. Basic Principles of Computational Fluid Dynamics [M]. Beijing: Science Press, 2001(in Chinese)

Author

Hu Dapeng, male, born in 1963, professor of Dalian University of Technology, Dean of the Department of Chemical Machinery. His current interests include unsteady-state flow and related equipment technology, and special chemical equipment technology. He has published about 20 papers, and achieved the rights of four patents. He has been awarded 2 national and 3 provincial prizes of science and technology. He can be reached by E-mail: hudapeng_dlut@ yahoo. com. cn

Foundation item: Chinese 863 National Program Foundation (No. 2006AA05Z216)